522 | Juni 1992

SCHRIFTENREIHE SCHIFFBAU

H. Petershagen

Fatigue Tests with Hyperbaric Dry Butt Welded Specimens

TUHH
Technische Universität Hamburg-Harburg

Fatigue Tests with Hyperbaric Dry Butt Welded Specimens

H. Petershagen, Hamburg, Technische Universität Hamburg-Harburg, 1992

Schriftenreihe Schiffbau
Schwarzenbergstraße 95c
D-21073 Hamburg

http://www.tuhh.de/vss

INSTITUT FÜR SCHIFFBAU DER UNIVERSITÄT HAMBURG

Bericht Nr. 522

FATIGUE TESTS WITH HYPERBARIC DRY BUTT WELDED SPECIMENS

H. PETERSHAGEN

Juni 1992

1. Introduction

In the investigation described in this report the repair of a surface crack at the toe of a butt weld unter hyperbaric conditions was simulated and the fatigue properties of the repaired weld have been studied. This study is part of the work in a research project "Damage investigation and prevention in underwater structures". The project is supported by Deutsche Forschungsgemeinschaft (DFG).

2. Fabrication of test specimens

The specimens were fabricated from a 20 mm thick rolled plate with the dimensions 8000 mm x 2000 mm. The material was Al-killed steel St 52-3 according to DIN 17 100. Chemical composition and mechanical properties are given in table 1. The material was selected because it has a less favourable weldability compared with more recently developed steel qualities, but is often found in existing offshore structures.

From the large plate smaller plates (500 mm x 240 mm) were cut by means of flame cutting. From these 500 mm x 480 mm large test plates were welded by means of the submerged arc process.

Fig. 1 shows the edge preparation and table 2 the welding parameters. After completion of the top side welding the root was chipped and rewelded. The average angular distortion of the completed weld was about 1° with only small scatter.

In the next step the groove for the repair weld (fig. 2) was prepared by milling. According to the situation often found in practice in the repair of a surface crack a groove depth of about half plate thickness was selected according to discussions with experts of Germanischer Lloyd.

The repair weld was carried out under dry hyperbaric conditions in the pressure chamber of the Laboratorium für Werkstoffkunde und Schweißtechnik der Universität der Bundeswehr Hamburg (Prof. Hoffmeister) under a pressure of 16 bar. The MIG-Pulsarc process was used for welding. The welding parameters were selected with regard to avoidance of weld defects and optimisation of the weld shape. Welding parameters and sequence of layers are given in table 3 and fig. 3.

3. Preparation for fatigue testing

In the Institut für Schiffbau der Universität Hamburg 50 mm wide test specimens were separated from the welded test plates by saw cut.

The specimens were measured in the device shown in fig. 4. From the distances d1 to d4 between the surface of the specimen and a reference line angular distortion and misalignment were calculated using the equations given in fig. 4 according to /1/(table 4). The secondary bending stresses were then calculated from equations given in /2/ and in fig. 4.

The maximum misalignment was found to be 0.9 mm with a much lower average. The misalignment can hence be considered as small. On the other hand, angular distortions between 1° and 4.5° were found. Maximum value as well as scatter are high. No explanation can be given especially for the high scatter. The situation with respect to angular distortion was at first considered as a disadvantage, but offered the opportunity of additional statements during the evaluation of test results.

Strain gauges of the type Hottinger LY6-120 were glued to one specimen from each test plate. The arrangement of strain gauges is shown in fig. 5. For the experimental investigation of residual stresses by means of the drilling hole method strain gauges TEA-06-062RK-120 were arranged at one specimen.

4. Fatigue testing

The fatigue tests were performed at a resonance machine Schenck PHX 60. In order to eliminate the influence of angular distortion of the specimens on the stress ratio, the specimens were clamped with the saw-cut edge upside.

The specimens with strain gauges were statically loaded prior to the fatigue test. The maximum stress under static load did not exceed that under the subsequent fatigue load. Linearity between load and strain and stability of strain gauge signal at zero load were checked by multiple stepwise loading.

The fatigue tests were carried out in air with a test frequency of about 30 Hz during resonance operation and about 2 Hz during hydraulic operation. The testing machine was operated hydraulically during the high load steps of the block program test only.

The test program included constant amplitude load tests with stress ranges of R=0 and R=-1 at two load levels each, a stair case test for 2 million cycles under zero - to tension load and 8-step block program tests according to Gassner under alternating load (R=-1). The exponential load distribution (/3/p.28) corresponds to the typical long-term distribution for offshore structures in the North Sea. Load data are given in table 10.

The number of specimens in the constant amplitude tests was at least 8 per load level. This is sufficient to justify a statistical analysis of the test results. Specimens from different test plates were combined for each test series resulting in a scatter of geometrical imperfections within each load level.

Drilling of the holes for the residual stress measurements was carried out by means of a device of Messrs. Measurements Group GmbH.

5. Test evaluation and results

5.1 Secondary bending stresses

The data from the strain gauge measurements are given in table 4. In order to compare calculated and measured bending stresses, the former had to be converted to those at the mid-point of the strain gauges. In the present case of a negligible influence of misalignment (see table 4) the point of zero bending moment lies at l/2 and the correction factor for the bending stresses calculated according to table 4 becomes

$$CF = \frac{l/2}{l/2+b} = \frac{1}{1+2b/l} = 0{,}72$$

with l = 127 mm and b = 25 mm.

A comparison of calculated and measured stresses (table 5 and fig. 6) shows good agreement. Only in two cases a deviation of 5% is slightly exceeded. Because of the smaller efforts and costs involved it is recommended to calculate the geometrical imperfections and secondary bending stresses in small-scale specimens loaded in tension according to the procedure given in table 4.

5.2 Residual stresses

In order to obtain the order of magnitude of residual stresses, drilling hole measurements were carried out at speciment no. 10.7.

The strain gauge arrangement is shown in fig. 7, details of evaluation and results in table 6.

At the repair weld side tensile residual stresses between 33% and 61% of the yield stress of the base material have been found. At the lower side a lower value of 23% of the yield stress was measured. With regard to the welding sequence these values appear reasonable. Parallel to the weld only small residual compression stresses were found.

5.3. Constant amplitude load fatigue tests

In most cases the crack initiated at the transition between repair weld and base material. Only these cases were used in the statistical evaluation. In some cases the crack initiated at the toe of the original weld. The data from these tests have been considered separately.

The test data are given in table 7, the results of the evaluation in table 8. The statistical evaluation for the individual stress levels was carried out under the usual assumption of a Gaussian distribution of fatigue lifes. An example is shown in fig. 8.

Figs. 9 and 10 show S-N curves for stress ranges R=0 and R=-1. The data are given in table 8. The stress ranges for 2 million cycles were obtained by extrapolation. The scatter band at each stress level corresponds to the ratio of fatigue lifes for 90% and 10% probability of survival.

A slope coefficient of about 3 has been found for both stress ranges investigated. This value, which is also used in codes as /4/ and /5/ is rather low for butt welds.

The significant nominal stress ranges for 2 million cycles are low compared with the scatter bands from the systematic re-analysis of test data /6/ as shown in fig. 11. This is at least partly due to the high secondary bending stresses caused by angular distortion. On the other hand, in spite of a considerable scatter of bending stresses, the scatter in the number of cycles to fracture for each individual test series ranges from 1 : 1,7 to 1 : 2,6 and is thus within usual limits. The effect of the stress ration is smaller than that found in /6/ (fig. 11). This corresponds with the residual stress state observed.

For a better comparison of the results with the scatter band in /6/ the data from the present investigation were converted to a common level of secondary bending stresses. According to /7/ the level of secondary bending stresses in existing test data is up to about 30% of the membrane stress. Assuming a slope of 3 for each individual specimen the fatigue lifes have been corrected to a common stress range of 1,30 x σ_m by means of the following equation.

$N_{corr} = N\ [\ (1+\sigma_b/\sigma_m)/1.30\ ]^3$
σ_b = secondary bending stress
σ_m = membrane stress
N = number of cycles to fracture in the test
N_{corr} = corrected number of cycles to fracture

The N_{corr} data are given in table 7 and the data for the corresponding S-N curves in table 8.

As fig. 11 shows, the stress ranges are still below the scatter band in /6/. Only if the stress range is based on membrane plus full bending stress, the stress ranges from the present investigation are close to the 50% (R=0) and 90% (R=-1) values according to /6/.

According to /4/ and /5/ the repair weld investigated would be classified as a class 80 detail based on membrane stress only. This classification is obtained from the stress range for 2 million cycles, 50% probability of survival and R=0 minus two standard deviations (1 standard deviation = factor 1,12 /8/). However, based on a common ratio of secondary bending stress and membrane stress of 1,30, the repair butt weld can be classified as a class 90 detail.

As table 8 shows, the slopes for the S-N lines from the data corrected for 30% secondary bending are slightly higher than for the lines based on membrane stress only. As could be expected, the scatter is reduced in all cases. This is also evident from figs. 12 and 13, which show scatter bands inluding all test data.

In fig. 12 also the data for specimens fractured at the toe of the initial weld are plotted. They fit very well into the scatter band of data from specimens, which failed from the repair weld toe.

5.4 Staircase test

The staircase test is a method for the assessment of the stress range for a given number of cycles (in the present case 2 million cycles) within given confidence limits. The first specimen is tested at an estimated stress range. If the number of cycles prescribed is reached without fracture, the following specimen is tested at an increased load level. If fracture occurs, the load level for the next test is reduced. A fixed ratio between adjacent load levels has to be chosen (in the present case 1,06). The test was carried out for a stress ratio R=O and the membrane stress was used as the nominal stress. Again specimens from different test plates were selected for the test. The sequence of specimens tested is shown in fig. 14.

The test data have been evaluated by an improved method described in /9/. In this method not only the fractured or non-fractured specimens but all data plus one additional information are used. Details of the evaluation are given in table 9.

A mean stress range of 117 N/mm^2 is obtained from the test, which is about 22% higher than the stress range of 96 N/mm^2 from the extrapolation of the sloped part of the S-N curve. For 90% probability of exceedance a stress range of 73 N/mm^2 has been calculated. The unusually high ratio between mean and p=90% value of 1,6 can be attributed to the scatter of angular distortion between the specimens tested. The highest stress level during the whole test (specimen no. 10,2) was reached, because the preceding specimen (no. 6,5) had a small angular distortion and hence small secondary bending stresses. On the contrary the lowest stress level (specimen no. 4,5) was reached by testing of a specimen with large angular distortion (no. 10.8) at the second lowest stress level. If the four specimens mentioned are omitted in the evaluation, a reasonable ration of 1,21 between mean and P = 90% value of stress ranges is obtained, while the mean value remains practically unchanged. The influence of scatter in the angular distortion on the results of the staircase test is obviously more pronounced than on the results of tests with constant amplitude load.

In order to get additional information, the non-fractured specimens were further tested after having reached 2 million cycles. During the continued test the stress range remained unchanged or was increased to 160 N/mm2. The results are plotted in fig. 15 together with the data from specimens fractured during the staircase test.

The data from the fractured specimens fit, with three exceptions, into the scatter band from the constant amplitude load test. A similar situation has been found for the specimens tested at an increased stress range. Only one of these specimens failed at a number of cycles below the scatter band. It can be concluded that the two other specimens were not considerably damaged during the staircase test. In all three cases where the number of cycles remained below the scatter band the angular distortion was higher than the average (see fig. 15).

The specimens tested at an unchanged stress range after 2 million cycles fractured at numbers of cycles up to about 4 million cycles. In cases, where run-outs are indicated in fig. 15, the specimens fractured at the toe of the submerged are weld or at the clamps. Mean line from constant amplitude load test and results from the staircase test indicate a knee in the S-N curve closely to 1 million cycles.

5.5 Block program test

Load sequence and test results are given in tables 10 and 11. Four data from specimens fractured at the toe of the repair weld are available. Cracks have also been observed at the toe of the submerged arc weld in all cases. A mean life of 3,766 million cycles was found with a ratio of 1,5 between highest and lowest number of cycles. A damage calculation was carried out. Details are shown in table 12. In this calculation Miner's rule was used with a slope of 3,11 below and 5,22 above 2 million cycles. The damage sum calculated is close to unity.

6. Calculations according to the notch stress concept

For eight specimens from different test plates calculations according to the notch stress concept /10/ have been carried out. Sections transverse to the weld have been cut from the specimens. The sections were amplified optically with a magnification factor of 10 and the relevant notch data taken (table 13). An example of a weld contour is shown in fig. 16.

For the calculation the contour was simplified as also shown in fig. 16. The modification includes the increase of notch root radius by 1mm proposed in /10/ to take account of the elastic stress field around the notch.

The calculation model is shown in fig. 17. No angular distortion is considered in the model. The stress analysis was carried out by means of the boundary element program BETSY.

An example for the stress distribution is shown in fig. 17. The results of all calculations are given in table 13. A mean stress range of 144 N/mm2for 2 million cycles and p = 90% probability of survival is obtained. This figure can be compared with the stress range of 150 N/mm2 from fig. 11 for zero-to-tension load with secondary bending stresses excluded. This figure is related to p = 50%. Converted to p = 90% (Factor 1/1.121.3 ; 1.12=factor for standard deviation /8/) $\Delta\sigma$ =129 N/mm2 is obtained. This is 11% below the mean calculated stress range. However, in the light of the result of the staircase test the extrapolation of the sloped part of the S-N curve seems to underestimate the stress range for 2 million cycles.

A mean value of K_F=1,80 is calculated from the data in table 13. This is slightly lower than K_F-values obtained for butt welds in other investigations /11/. It should, however, be kept in mind that the present calculations were carried out with the really existing root radii plus 1 mm and not, as proposed in /10/ with a geometrical root radius of zero.

It can, however, be concluded from the calculation that the shape of the repair welds investigated is not inferior to that of usual butt welds.

7. Summary

Butt welds with hyperbaric dry MIG-repair welds have been tested under axial fatigue load.

The secondary bending stresses due to geometrical imperfection can be derived from simple measurements.

Residual tensile stresses of about 30-60% of the yield stress were measured perpendicular to the weld.

The slope of S-N curves for stress rations R=O and R=-1 is about 3, the knee of the curve is located closely to 1 million cycles. The stress range for 2 million cycles is comparatively low. As experiments as well as calculations according to the notch stress method show, this is mainly due to the comparatively high angular distortion and not to an inferior weld shape. With angular distortions corresponding to a ratio between secondary bending stress and membrane stress of 1,30 the repair weld can be classified as a class 90 detail according to the IIW Fatigue Design Recommendation /4/.

Results from block program tests fit well with a damage calculation using Miner's rule.

Most specimens fractured from the toe of the repair weld. However, fracture or at least crack initiation was also observed at the toe of the initial submerged arc weld. From this it can be concluded that the fatigue properties of original and repair weld are nearly equivalent.

References

/1/ Fatigue testing of welded components
IIW-Document XIII-WG1-29-91, 1991

/2/ H. Petershagen und W. Zwick
Fatigue strength of butt welds made by different welding processes
IIW-Document XIII-1048-82, 1982

/3/ O. Buxbaum
Betriebsfestigkeit - sichere und wirtschaftliche Bemessung schwingbruchgefährdeter Bauteile
(Fatigue strength - safe and economical design of structures prone to fatigue failure)
Verlag Stahleisen mbH Düsseldorf 1986

/4/ Design recommendations for cyclic loaded welded steel structures
Welding in the World Vol. 20 No. 7/8, 1982, p. 153

/5/ Eurocode 3 Design of Steel Structures
Part 1 - General Rules and Rules for Buildings
Section 9 Fatigue
Edited draft, issue 3, April 1990

/6/ R. Olivier und W. Ritter
Catalogue of S-N-curves in structural steels
Part 1: Butt joints
DVS Report No. 56/I

Deutscher Verlag für Schweißtechnik GmbH
Düsseldorf 1979

/7/ S.J. Maddox
Fitness-for-purpose assessment of misalignment
in transverse butt welds subject to fatigue loading
IIW-Document XIII-1180-85, 1985

/8/ IIW-JWG-XIII-XV Doc. No. 34-78, 1978
Ranking of the different notch cases
for the proposed fatigue design rules

/9/ M. Hück
An improved method for the evaluation of
staircase tests
Zeitschrift für Werkstofftechnik 14/1983 p. 406

/10/ D. Radaj
Design and analysis of fatigue
resistant welded structures
Abington Publishing 1990
Abington, Cambridge CB1 6AH England

/11/ H. Petershagen
Erfahrungen mit dem Kerbspannungskonzept
nach Radaj (experiences with the notch
stress concept according to Radaj)
in "Kerben und Betriebsfestigkeit"
15. Vortragsveranstaltung des DVM -
Arbeitskreis Betriebsfestigkeit
Ingolstadt 1989, p. 89

Table 1 Base Material

Chemical Composition in %

C	Si	Mn	P	S	Al	Nb	V
0.18	0.38	1.47	0.016	0.006	0.036	0.020	0.004

Mechanical Properties

REH N/mm^2	RM N/mm^2	ISO-V-Notch Toughness Joule at 20°C				
405	580	146	154	136	mean	145

Table 2 Submerged Arc Welding Parameters

Layer	Current A	Voltage V	Wire Speed mm/min
1 Root Layer	5oo	27	700
2 Intermediate Layer	600	30	500
3 Counter Layer	600	34	500
4 Top Layer	600	34	500

Wire: S 2 Mo 4 mm
Powder: L W 320
Powder Height 22 mm

Table 3 Repair Welding Parameters

Pressure	16 bar		
Puls Voltage	54 V		
Puls Current	280 A		
Puls Cycle	4,7 ms		
Base Voltage	15 V		
Base Current	50 A		
Base Cycle	5,0 ms		
Wire Diameter	1,0 mm		
Wire Speed	9,8 m/min		
Weld Speed	Layer 1	387 mm/min	
	" 2	285 mm/min	
	" 3	285 mm/min	
	" 4	387 mm/min	

Gas Flow	Ar	112,5 Nl/min
	ArS3	7,5 Nl/min

Table 4.1 Geometric Imperfections

Plate No. 2 l= 129 mm b= 25 mm

Spec No.	d_1 [mm]	d_2 [mm]	d_3 [mm]	d_4 [mm]	e [mm]	φ [°]	$\frac{\sigma_{b2}}{\sigma_m}$	$\frac{\sigma_{b3}}{\sigma_m}$
2.1	20,07	15,67	15,07	20,95	0,83	-3,68	0,44	0,80
2	20,25	15,73	15,28	21,00	0,64	-3,67	0,47	0,76
3	20,20	15,63	15,18	20,91	0,63	-3,69	0,48	0,76
4	20,20	15,64	15,20	20,89	0,62	-3,67	0,48	0,76
5	20,30	15,58	15,30	20,85	0,41	-3,68	0,52	0,72
6	20,25	15,68	15,38	20,85	0,44	-3,60	0,50	0,72
7	20,16	15,65	15,25	20,84	0,57	-3,62	0,48	0,74
8	20,23	15,63	15,18	20,87	0,62	-3,68	0,49	0,75

Plate No. 3 l= 127 mm b= 25 mm

Spec No.	d_1 [mm]	d_2 [mm]	d_3 [mm]	d_4 [mm]	e [mm]	φ [°]	$\frac{\sigma_{b2}}{\sigma_m}$	$\frac{\sigma_{b3}}{\sigma_m}$
3.1	27,10	20,85	20,90	26,95	-0,08	-4,40	0,76	0,70
2	27,00	20,85	20,90	26,95	-0,07	-4,37	0,74	0,71
3	26,90	20,90	20,85	26,85	+0,05	-4,30	0,71	0,71
4	26,95	20,90	20,73	26,80	+0,17	-4,34	0,72	0,72
5	27,00	21,00	20,80	26,70	+0,18	-4,26	0,72	0,69
6	26,70	21,13	20,70	26,55	+0,47	-4,09	0,65	0,71
7	27,03	20,80	20,85	26,80	-0,09	-4,36	0,76	0,69
8	27,00	20,80	20,80	26,87	-0,02	-4,39	0,75	0,71

Table 4.2

Plate No.4 l= 126 mm b= 25 mm

Spec No.	d_1 [mm]	d_2 [mm]	d_3 [mm]	d_4 [mm]	e [mm]	φ [°]	$\frac{\sigma_{b2}}{\sigma_m}$	$\frac{\sigma_{b3}}{\sigma_m}$
4.1	25,85	21,52	21,12	25,47	0,40	-3,11	0,51	0,52
2	26,00	21,58	21,10	26,17	0,58	-3,40	0,48	0,64
3	25,95	21,63	21,28	26,15	0,44	-3,29	0,48	0,61
4	25,87	21,49	21,20	26,10	0,37	-3,32	0,49	0,61
5	25,90	21,40	21,15	36,12	0,32	-3,39	0,50	0,61
6	25,82	21,35	21,16	26,10	0,26	-3,37	0,50	0,61
7	25,72	21,30	21,18	26,19	0,21	-3,38	0,49	0,63
8	25,98	21,28	21,00	26,10	0,34	-3,51	0,53	0,63

Plate No.5 l= 127 mm b= 25 mm

5.1	25,12	22,60	22,10	26,13	0,74	-2,35	0,21	0,57
2	25,25	22,50	22,10	26,10	0,59	-2,42	0,25	0,55
3	25,20	22,50	22,00	26,15	0,73	-2,45	0,24	0,58
4	25,30	22,49	22,00	26,32	0,73	-2,55	0,24	0,60
5	25,40	22,55	22,05	26,40	0,73	-2,58	0,25	0,60
6	25,45	22,48	21,95	26,35	0,75	-2,64	0,27	0,60

Plate No.6 l= 126,5 mm b= 25 mm

6.1	25,75	22,60	22,22	25,40	0,38	-2,27	0,37	0,38
2	25,65	22,65	22,45	25,27	0,17	-2,08	0,37	0,32
3	25,40	22,90	22,52	25,30	0,42	-1,89	0,28	0,35
4	25,20	23,05	22,58	25,20	0,54	-1,71	0,23	0,34
5	25,15	23,20	22,61	25,20	0,69	-1,63	0,19	0,35
6	25,15	23,20	22,65	25,15	0,64	-1,59	0,20	0,33
7	25,10	23,24	22,65	25,35	0,72	-1,63	0,17	0,37
8	24,94	23,35	22,55	25,48	1,00	-1,62	0,11	0,43
9	25,00	23,25	22,46	25,52	0,99	-1,72	0,13	0,44

Plate No.7 l= 126,5 mm b= 25 mm

7.1	19,85	16,53	16,40	19,75	0,13	-2,39	0,39	0,40
2	19,80	16,48	16,40	19.75	0,08	-2,39	0,39	0,40
3	19,70	16,58	16,48	19,70	0,12	-2,27	0,36	0,39
4	19,75	16,55	16,42	19,82	0,16	-2,36	0,37	0,42
5	19,70	16,50	16,35	19,78	0,19	-2,37	0,37	0,42
6	19,73	16,50	16,50	19,79	0,01	-2,33	0,38	0,39
7	19,82	16,20	16,45	19,87	-0,28	-2,52	0,44	0,39
8	19,82	16,30	16,30	19,93	0,02	-2,56	0,41	0,44

Table 4.3

Plate No.8 l= 126 mm b= 25 mm

Spec No.	d_1 [mm]	d_2 [mm]	d_3 [mm]	d_4 [mm]	e [mm]	φ [°]	$\frac{\sigma_{b2}}{\sigma_m}$	$\frac{\sigma_{b3}}{\sigma_m}$
8.1	26,35	21,87	21,35	26,12	0,57	-3,31	0,51	0,58
2	26,18	21,67	21,20	25,85	0,49	-3,28	0,52	0,56
3	26,15	21,80	21,58	25,55	0,16	-2,98	0,54	0,44
4	26,12	22,00	21,70	25,95	0,32	-3,00	0,48	0,51
5	26,10	22,10	21,75	26,05	0,40	-2,97	0,45	0,53
6	26,12	22,00	21,67	25,90	0,35	-2,99	0,48	0,51
7	26,12	22,08	21,80	26,10	0,32	-2,99	0,46	0,52
8	26,08	22,00	21,70	25,82	0,31	-2,94	0,48	0,49

Plate No. 9 l= 126,5 mm b= 20 mm

Spec No.	d_1 [mm]	d_2 [mm]	d_3 [mm]	d_4 [mm]	e [mm]	φ [°]	$\frac{\sigma_{b2}}{\sigma_m}$	$\frac{\sigma_{b3}}{\sigma_m}$
9.1	19,44	17,06	16,71	20,00	0,46	-2,03	0,23	0,45
2	19,23	16,90	16,63	20,50	0,46	-2,22	0,19	0,55
3	19,19	16,47	16,43	20,00	0,15	-2,25	0,27	0,48
4	19,25	16,80	16,63	19,80	0,26	-2,01	0,25	0,42
5	19,35	17,00	16,53	19,78	0,58	-2,00	0,23	0,44
6	19,27	17,02	16,65	19,50	0,45	-1,83	0,23	0,38
7	19,37	17,03	16,89	19,73	0,20	-1,85	0,25	0,37
8	19,24	16,90	16,76	19,75	0,22	-1,91	0,24	0,40
9	19,40	17,00	16,79	19,95	0,31	-1,99	0,24	0,42

Plate No. 10 l= 126,5 mm b= 25 mm

Spec No.	d_1 [mm]	d_2 [mm]	d_3 [mm]	d_4 [mm]	e [mm]	φ [°]	$\frac{\sigma_{b2}}{\sigma_m}$	$\frac{\sigma_{b3}}{\sigma_m}$
10.1	26,35	21,65	21,23	26,65	0,53	-3,62	0,51	0,68
2	26,40	21,63	21,25	26,70	0,49	-3,66	0,53	0,68
3	26,36	21,67	21,23	26,74	0,57	-3,65	0,51	0,70
4	26,32	21,70	21,35	26,65	0,46	-3,55	0,51	0,67
5	26,25	21,60	21,23	26,88	0,53	-3,69	0,49	0,73
6	26,60	21,35	20,85	27,10	0,66	-4,12	0,56	0,80
7	26,35	21,53	21,13	26,95	0,55	-3,81	0,51	0,75
8	26,53	21,40	21,05	26,95	0,47	-3,95	0,56	0,74

Plate No. 11 l= 126,5 mm b= 25 mm

Spec No.	d_1 [mm]	d_2 [mm]	d_3 [mm]	d_4 [mm]	e [mm]	φ [°]	$\frac{\sigma_{b2}}{\sigma_m}$	$\frac{\sigma_{b3}}{\sigma_m}$
11.1	18,65	17,60	17,39	19,20	0,33	-1,02	0,08	0,26
2	18,60	17,40	17,00	19,08	0,54	-1,17	0,09	0,30
3	18,61	17,68	17,02	19,08	0,84	-1,07	0,04	0,31
4	18,59	17,48	17,02	19,00	0,60	-1,11	0,08	0,29
5	18,40	17,68	17,00	19,00	0,88	-0,97	0,01	0,31
6	18,50	17,70	16,95	18,90	0,93	-0,98	0,03	0,30

Table 4.4

Plate No. 14 l= 128 mm b= 25 mm

Spec No.	d_1 [mm]	d_2 [mm]	d_3 [mm]	d_4 [mm]	e [mm]	φ [°]	$\frac{\sigma_{b2}}{\sigma_m}$	$\frac{\sigma_{b3}}{\sigma_m}$
14.1	23,15	21,26	21,06	23,60	0,30	-1,58	0,19	0,34
2	23,22	21,60	21,20	23,60	0,52	-1,44	0,15	0,33
3	23,20	21,30	21,05	23,50	0,34	-1,56	0,20	0,33
4	23,25	21,40	21,10	23,62	0,40	-1,56	0,18	0,34
5	23,15	21,30	21,08	23,60	0,32	-1,56	0,18	0,34
6	23,27	21,25	21,15	23,55	0,16	-1,58	0,22	0,31
7	23,50	21,30	21,00	23,60	0,36	-1,72	0,24	0,34
8	23,55	21,00	21,25	23,60	-0,28	-1,75	0,32	0,27
9	23,52	21,10	21,15	23,65	-0,04	-1,76	0,29	0,30

Table 5 Measured vs. calculated bending stress

Spec No.	mean stress σ_m [N/mm^2]	measured strains $\cdot 10^{-6}$ ε_1	ε_2	ε_3	ε_4	relative bending stresses σ_{b2} / σ_m meas.	σ_{b2} / σ_m cacl.	σ_{b3} / σ_m meas.	σ_{b3} / σ_m cacl.
2.6	232	658	1515	1627	527	0,39	0,36	0,51	0,52
3.4	100	210	750	778	215	0,56	0,52	0,57	0,52
4.5	100	268	639	689	237	0,41	0,36	0,49	0,44
5.6	100	336	578	665	271	0,26	0,19	0,42	0,43
6.9	100	416	521	631	327	0,11	0,09	0,32	0,32
7.2	232	745	1438	1508	739	0,32	0,28	0,34	0,29
8.4	100	303	538	694	282	0,28	0,35	0,42	0,37
9.6	232	859	1349	1467	789	0,22	0,17	0,30	0,27
10.8	100	262	694	755	207	0,45	0,40	0,57	0,53
11.2	232	1000	1176	1380	860	0,08	0,06	0,23	0,22
14.9	100	342	588	607	362	0,26	0,21	0,25	0,22

strain gauge arrangement see fig.5

Table 6 Results of residual stress measurements

$D = 5,13mm$

$D_0 = 1,7\ mm$

$a = 0,14$

$b = 0,34$

$\nu = 0,3$

$$A = -\frac{1+\nu}{2E}\,a = -4,33\cdot 10^{-7}$$

$$B = -\frac{1}{2E}\,b = -8,10\cdot 10^{-7}$$

$$\tan 2\bar{\beta} = \frac{\varepsilon_1 - 2\varepsilon_2 + \varepsilon_3}{\varepsilon_3 - \varepsilon_1}$$

$$\beta = \bar{\beta} \quad \text{for} \quad \varepsilon_1 \geq \varepsilon_3$$

$$\beta = 90^\circ - \bar{\beta} \quad \text{for} \quad \varepsilon_1 \leq \varepsilon_3$$

$$\sigma_{\substack{x\\y}} = \frac{\varepsilon_1 + \varepsilon_3}{4A} \pm \frac{\sqrt{2}}{4B}\sqrt{(\varepsilon_1 - \varepsilon_2)^2 + (\varepsilon_2 - \varepsilon_3)^2}$$

Gauge No.	Strain · 10^{-6} ε_1	ε_2	ε_3	Stress [N/mm^2] σ_x	σ_y	β°
1	- 178	+ 3	+ 96	+ 136	- 42	- 9
2	- 154	- 146	+ 110	+ 137	- 86	+ 22
3	- 272	+ 90	+ 117	+ 248	- 69	- 20
4	- 131	- 26	+ 84	+ 94	- 39	+ 1

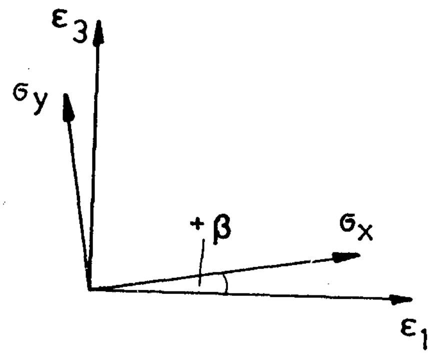

12

Table 7.1 Data from constant amplitude load tests

Series 01 R= 0 $\Delta\sigma_m$= 232 N/mm^2

Spec. No.	$\Delta\sigma_b / \Delta\sigma_m$	$\Delta\sigma_b + \Delta\sigma_m$ [N/mm^2]	N cycles	N_{corr} cycles	crack init. side
8.1	0,58	367	74400	133572	3*)
2.1	0,80	418	103200	273947	
9.7	0,37	318	120000	140447	
7.2	0,40	325	131000	163616	
9.6	0,38	320	154300	184575	
11.1	0,26	292	162900	148321	
11.2	0,30	302	174500	174500	
7.1	0,40	325	179900	224691	3
2.6	0,50	348	118700	182345	2*)
2.7	0,48	343	127700	188428	2

$$N_{corr} = N \cdot \left(\frac{1+\sigma_b/\sigma_m}{1,3}\right)^3$$

*2 crack at initial weld,
3 crack at repair weld

Series 02 R= 0 $\Delta\sigma_m$= 160 N/mm^2

Spec. No.	$\Delta\sigma_b / \Delta\sigma_m$	$\Delta\sigma_b + \Delta\sigma_m$ [N/mm^2]	N cycles	N_{corr} cycles	crack init. side
4.1	0,52	243	300500	480336	3
4.8	0,63	261	308800	608709	
8.2	0,56	250	337100	582509	
4.2	0,64	262	361400	725587	
11.6	0,30	208	438600	438600	
9.2	0,55	248	488900	828677	
9.1	0,45	232	559100	775824	
7.3	0,39	222	640000	782338	3
2.8	0,49	238	393800	592931	2
7.4	0,37	219	522500	611530	2

Table 7.2

Series 11 R=-1 $\Delta\sigma_m$= 160 N/mm^2

Spec. No.	$\Delta\sigma_b/\Delta\sigma_m$	$\Delta\sigma_b+\Delta\sigma_m$ [N/mm^2]	N cycles	N_{corr} cycles	crack init. side
4.7	0,63	261	508400	1002163	3
2.5	0,72	275	512400	1186764	
8.5	0,53	245	644900	1051324	
4.6	0,61	258	712700	1353799	
9.3	0,48	237	762400	1124962	
8,4	0,51	242	766400	1201037	
5.1	0,57	251	811400	1429236	
8.3	0,44	230	861700	1171153	3

Series 12 R= -1 $\Delta\sigma_m$= 240 N/mm^2

Spec. No.	$\Delta\sigma_b/\Delta\sigma_m$	$\Delta\sigma_b+\Delta\sigma_m$ [N/mm^2]	N cycles	N_{corr} cycles	crack init. side
3.8	0,71	410	108700	247393	3
9.9	0,42	341	145900	202455	
2.4	0,76	422	155400	385619	
14.1	0,34	322	194200	212683	
4.4	0,61	386	212000	402702	
14.6	0,31	314	246000	270139	
14.5	0,34	322	246800	270290	
6.8	0,43	346	306400	416434	3

Table 8 Results of constant amplitude load tests

a) Evaluation based on membrane stress σ_m only

	Series 01	Series 02	Series 11	Series 12
N_{10} cycles	198950	610102	896010	313590
N_{50} "	132541	414285	685793	194232
N_{90} "	88299	281317	524897	120303
N_{10}/N_{90}	1:2,3	1:2,2	1:1,7	1:2,6
K	3,07		3,11	

b) Evaluation based on membrane + 30% bendingstress $\sigma_m+\sigma_b$

	01	02	11	12
N_{10} cycles	244844	879027	1392238	426873
N_{50} "	175562	637472	1182714	290191
N_{90} "	125884	462296	1004721	197274
N_{10}/N_{90}	1:1,9	1:1,9	1:1,4	1:2,2
K	3,47		3,47	

$N_{10,(50),(90)}$ = Number of cycles for 10 (50) (90) % probability of survival

K = slope of S-N-curve

Table 9 Evaluation of staircase test
stress ratio R= 0

Spec. No.	$\Delta\sigma_b/\sigma_m$	$\Delta\sigma[N/mm^2]$	$\Delta\sigma_2[N/mm^2]$ 1) 2)	N_f
11.5	0,31	120,0		1389800
7.6	0,39	113,4 NF 1)	160,0	201300
9.8	0,40	120,0		1087800
11.4	0,29	113,4 NF		4068200
5.5	0,60	120,0		1199500
7.7	0,39	113,4 NF		4189600
6.2	0,32	120,0 NF	160,0	253200
6.3	0,35	127,0		1189600
6.4	0,34	120,0 NF		3126800 R 3)
6.5	0,35	127,0 NF		-
10.2	0,68	134,0		451900
10.1	0,68	127,0		599100
10.5	0,73	120,0		612200
10.3	0,70	113,4		1026800
9.5	0,44	107,2 NF	160,0	555900
10.4	0,67	113,4 NF		-
3.2	0,71	120,0		1005600
3.3	0,71	113,4		792700
8.6	0,51	107,2 NF		2353000 R
6.9	0,44	113,4 NF		3217800
3.4	0,72	120,0		471600
8.4	0,51	113,4		1366200
10.8	0,74	107,2		856900
4.5	0,61	101,2 NF		2880200
5.6	0,60	107,2 NF		2788300
14.9	0,30	103,4 NF		2863000 R
14.8	0,27	120,0 NF		2443800 R
14.2	0,33	127,0		1081400
14.3	0,33	120,0 NF		2331400
-	-	127,0 -	-	-

1) No fracture at 2 million cycles
2) Stress range after 2 million cycles
3) R= runout

Evaluation after /11/:

step i	number f_i	$i \cdot f_i$	$i^2 \cdot f_i$	stress range $\Delta\sigma[N/mm^2]$
0	1	0	0	101,2
1	4	4	4	107,2
2	9	18	36	113,4
3	10	30	90	120,0
4	5	20	80	127,0
5	1	5	25	134,0
	F=30	A=77	B=235	

Table 9.2

Step factor $d = 1,0583$ $\log d = 0,02461$

Mean stress range $\Delta\bar{\sigma} = \Delta\sigma_{ö}\ d^{A/F} = 101,2 \cdot 1,0583^{77/30} = 117,0\ N/mm^2$

Variance $K = \frac{F \cdot B - A^2}{F^2} = 1,2456$

Standard deviation /11/fig.15 $\log s = 0,02461 \cdot 2,3 = 0,05660$
$s = 1,139$

Confidence range 90% $K_1 = 1,28$

Standard error mean stress range $\log s_m = C_m \cdot \log s$

$$C_m = 0,23 \text{ (/11/ fig.16) for } \frac{\log s}{\log d} = \frac{0,05660}{0,02461} = 2,30$$

$\log s_m = 0,23 \cdot 0,05660 = 0,01302$
$s_m = 1,030$

Standard error standard deviation $\log s_s = C_s \cdot \log d$

$C_S = 2,80$ (/11/ fig.17)
$\log s_S = C_S \cdot \log d = 2,80 \cdot 0,02461 = 0,06891$
$S_S = 1,172$
$K_2 = 1,28$ for $p_{ü} = 90\%$

$$\log \Delta\sigma_{90} = \log \overline{\Delta\sigma} - K_2 \log s - K_1 \sqrt{(\log s_m)^2 + (K_2 \log s_s)^2}$$

$$= 2,0682 - 1,28 \cdot 0,05660 - 1,28 \sqrt{0,01302^2 + (1,28 \cdot 0,06891)^2}$$

$= 1,8816$
$\Delta\sigma_{90} = 76,1\ N/mm^2$
$\Delta\sigma_{90} / \Delta\bar{\sigma} = 0,65$

Evaluation after omission of specimens 6.5/10.2 and 10.8/4.5:

$\Delta\bar{\sigma} = 117,2\ N/mm^2$
$K = 0,7825$
$\log s = 0,03076$ $s = 1,073$
$\log s_m = 0,00846$ $s_m = 1,020$
$\log s_s = 0,02584$ $s_s = 1,061$
$\log \Delta\sigma_{90} = 1,9851$ $\Delta\sigma_{90} = 96,6\ N/mm^2$
$\Delta\sigma_{90} / \Delta\bar{\sigma} = 0,82$

Table 10 Block Program Test

Stress ratio R=-1
Load sequence

Step No.	No. of cycles	Stress range [N/mm^2]
4	87	387,5
3	15	465,0
2	3	542,5
1	1	620,0
2	3	542,5
3	15	465,0
4	87	387,5
5	487	310,0
6	2 730	232,5
7	15 400	155,0
8	462 000	77,5
7	15 400	155,0
6	2 730	232,5
5	487	310,0
	499 445	

Table 11 Results from block programm test

Spec. No.	N resonance	N hydr.	N total	
7.8	4 477 000	59 788	4 536 788	
4.3	3 458 700	49 456	3 508 156	
14.4	3 956 500	56 187	4 012 687	
2.2	2 963 500	42 907	3 006 407	
(12.1	1 976 300	29 758	2 006 058)	root crack

mean 3 766 000 cycles

Table 12 Damage accumulation calculation

failure criterion $$D \cdot \sum_{i=1}^{8} \frac{n_i}{N_i} = 1 \qquad (1)$$

D = number of blocks to fracture
n_i = number of cycles in step: per block (see below)
N_i = number of cycles to fracture in step: under constant amplitude load

$$\Delta\sigma_i = \Delta\sigma_{max} \left(1{,}125 - \frac{i}{8}\right) \qquad (2)$$

$\Delta\sigma_i$ = stress range for step i

$$N_i = 2 \cdot 10^6 \left(\frac{\Delta\sigma_i}{\Delta\sigma_D}\right)^{-K_i} \qquad (3)$$

σ_D = stress range for 2 million cycles under constant amplitude load

From (1) and (3)

$$D = \frac{1}{\sum_i \frac{n_i}{N_i}} = \frac{2 \cdot 10^6}{\sum_i n_i \left(\frac{\Delta\sigma_i}{\Delta\sigma_D}\right)^{K_i}}$$

$\Delta\sigma_D = 114\ N/mm^2$ $\qquad \Delta\sigma_{max} = 620\ N/mm^2$

step i	n_i	$\Delta\sigma_i$ N/mm^2	K_i	$n_i \left(\frac{\Delta\sigma_i}{\Delta\sigma_D}\right)^{K_i}$
1	1	620	3,11	194
2	6	543		770
3	30	465		2 376
4	174	388		7 849
5	974	310		21 863
6	5 460	233		50 431
7	30 800	155	3,11	80 077
8	462 000	78	5,22	63 728
	499 445			227 288

$$D = \frac{2 \cdot 10^6}{227\ 288} = 8{,}80$$

N_{calc} = 499 445 · 8,80 = 4 395 000

N_{calc}/N_{exp} = 4 395 000 / 3 766 000 = 1,17

Table 13 Results of notch stress calculations

Spec. No.	root radius [mm]	flank angle [°]	K_F	$\Delta\sigma_D$ [N/mm^2]
1.2	2,5	32	1,71	149
2.3	2,5	42	1,73	147
3.5	1,9	42	2,01	128
5.	1,8	30	1,97	130
6.4	4,4	24	1,56	163
7.7	5,4	26	1,52	166
10.6	1,5	47	2,25	115
14.8	4,3	28	1,64	155
			mean 1,80	mean 144

1) $\Delta\sigma_D = \Delta\sigma \ (N=2\cdot 10^6; p=90\% \ , R=0)$

$$\Delta\sigma_D = \frac{270}{K_F + 0,1}$$

25

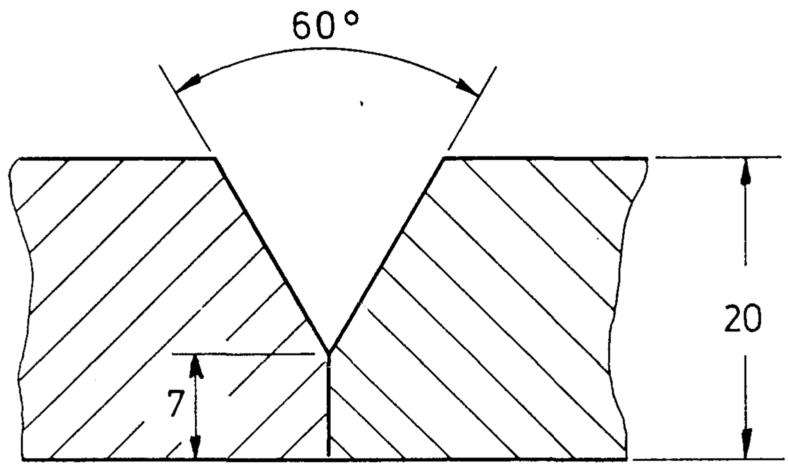

Fig. 1 Edge preparation for SAW butt weld

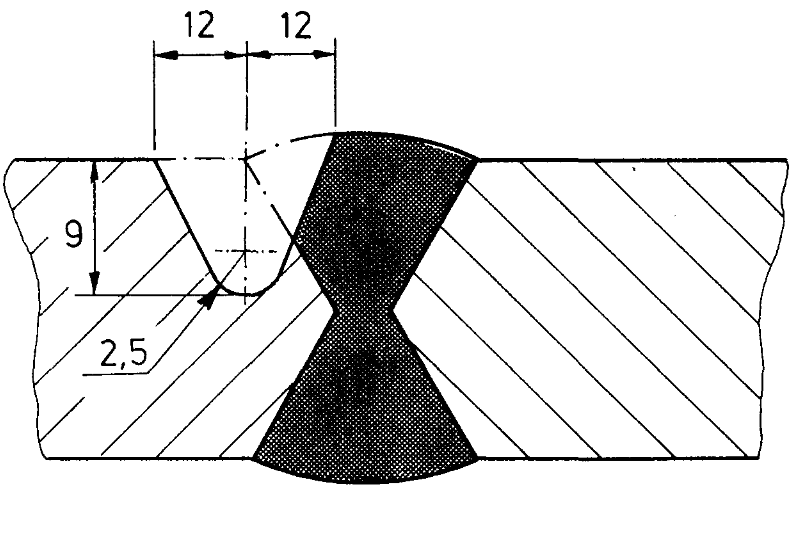

Fig. 2 Edge preparation for repair weld

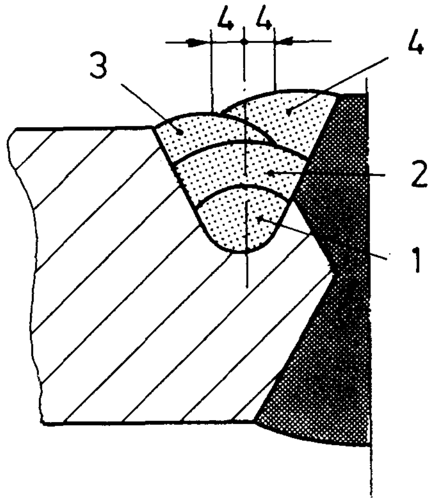

Fig. 3 Welding sequence repair weld

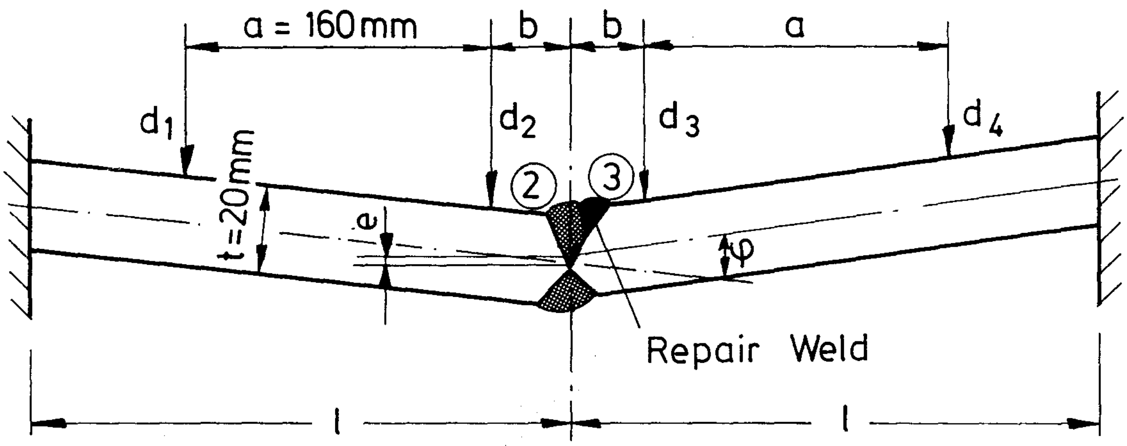

Misalignment: $e = (d_2 - d_3)(1 + \frac{b}{a}) + (d_4 - d_1)\frac{b}{a}$

Angular Distortion: $\varphi° = \frac{180}{\pi \cdot a}(d_2 - d_1 + d_3 - d_4)$

Rel. Bending Stresses :

Point 2 $\quad \frac{\sigma_{b2}}{\sigma_m} = -\frac{3l}{2at}[3(d_2 - d_1) - (d_3 - d_4)]$

Point 3 $\quad \frac{\sigma_{b3}}{\sigma_m} = +\frac{3l}{2at}[(d_2 - d_1) - 3(d_3 - d_4)]$

Fig. 4 Determination of geometrical imperfections

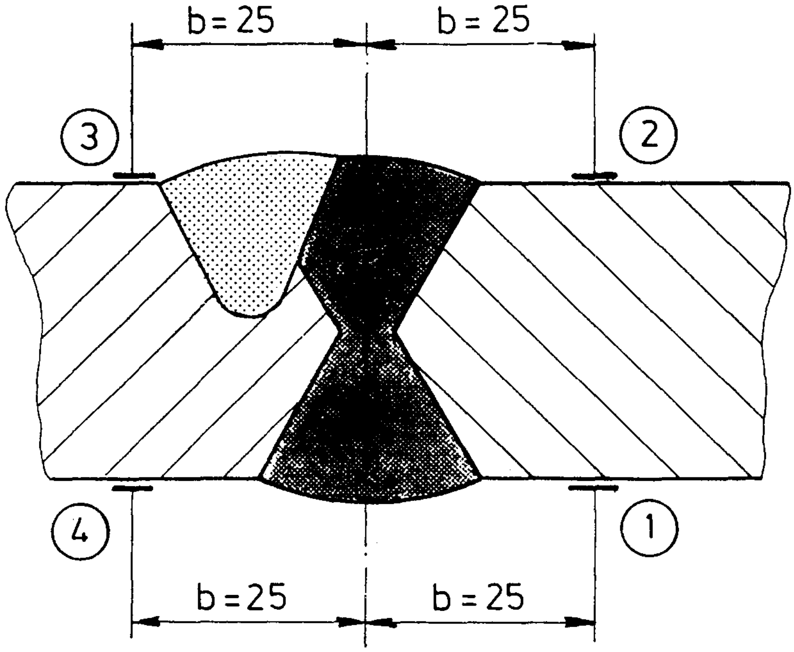

Fig. 5 Arrangement of strain gauges for secondary bending stress measurements

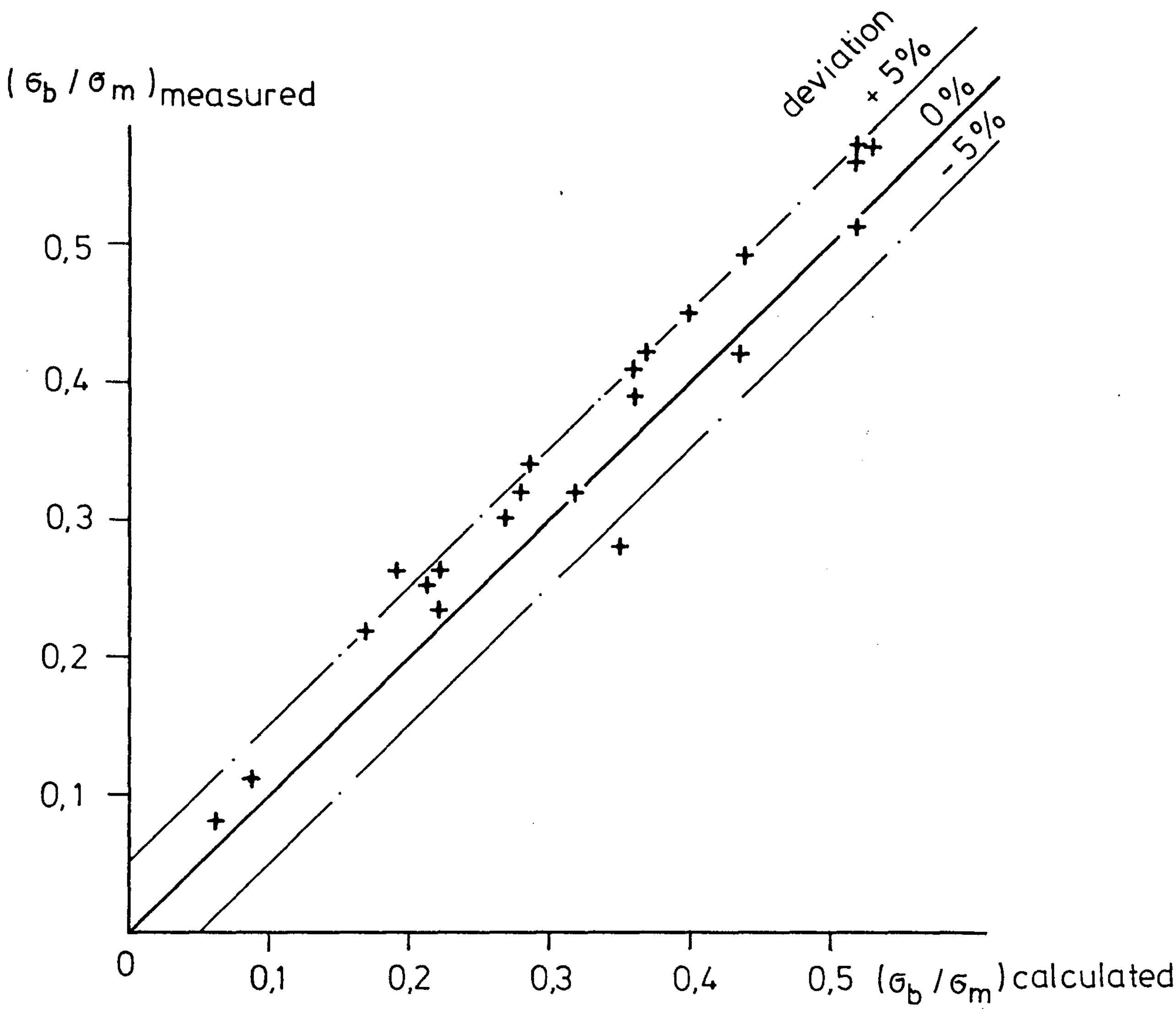

σ_m = membrane stress

σ_b = secondary bending stress

Fig. 6 Comparison of measured and calculated secondary bending stresses

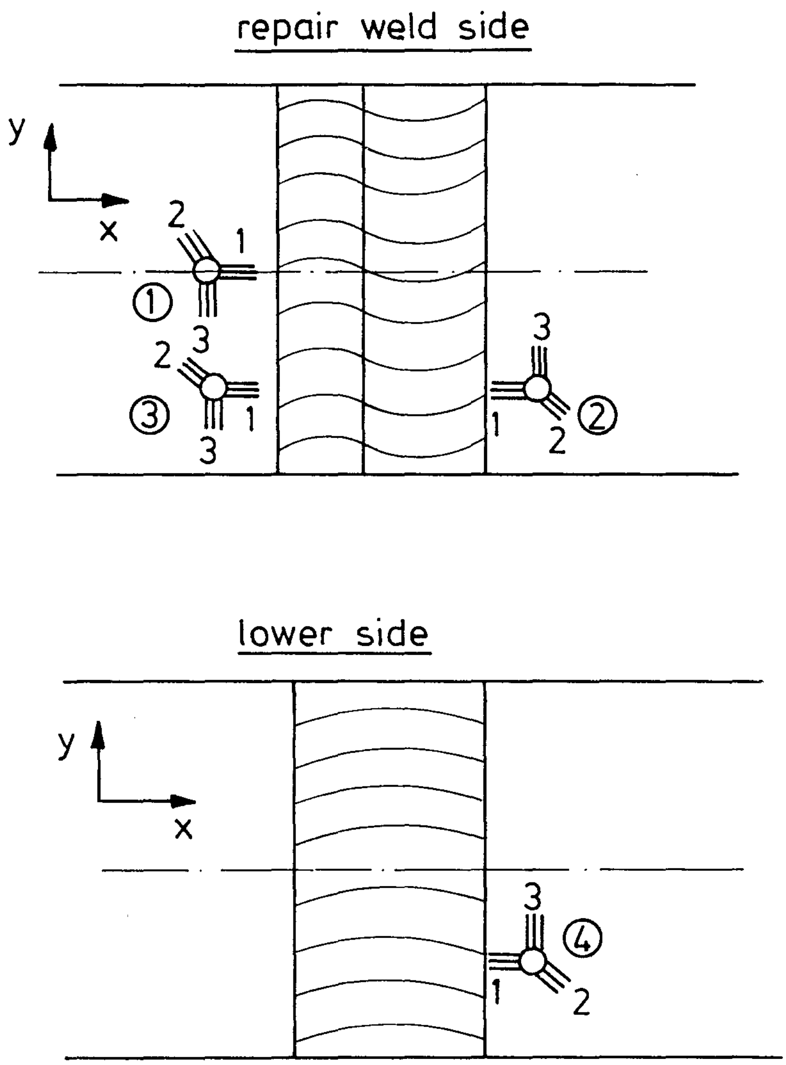

Fig. 7 Arrangement of strain gauges for residual stress measurements

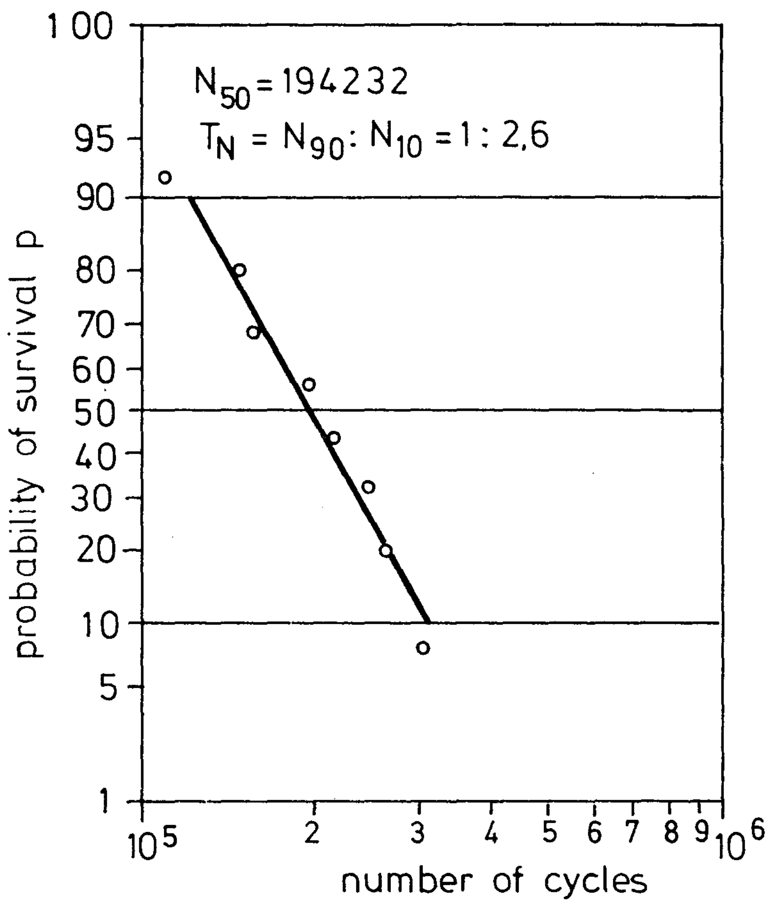

Fig. 8 Evaluation of constant amplitude load test (series 12)

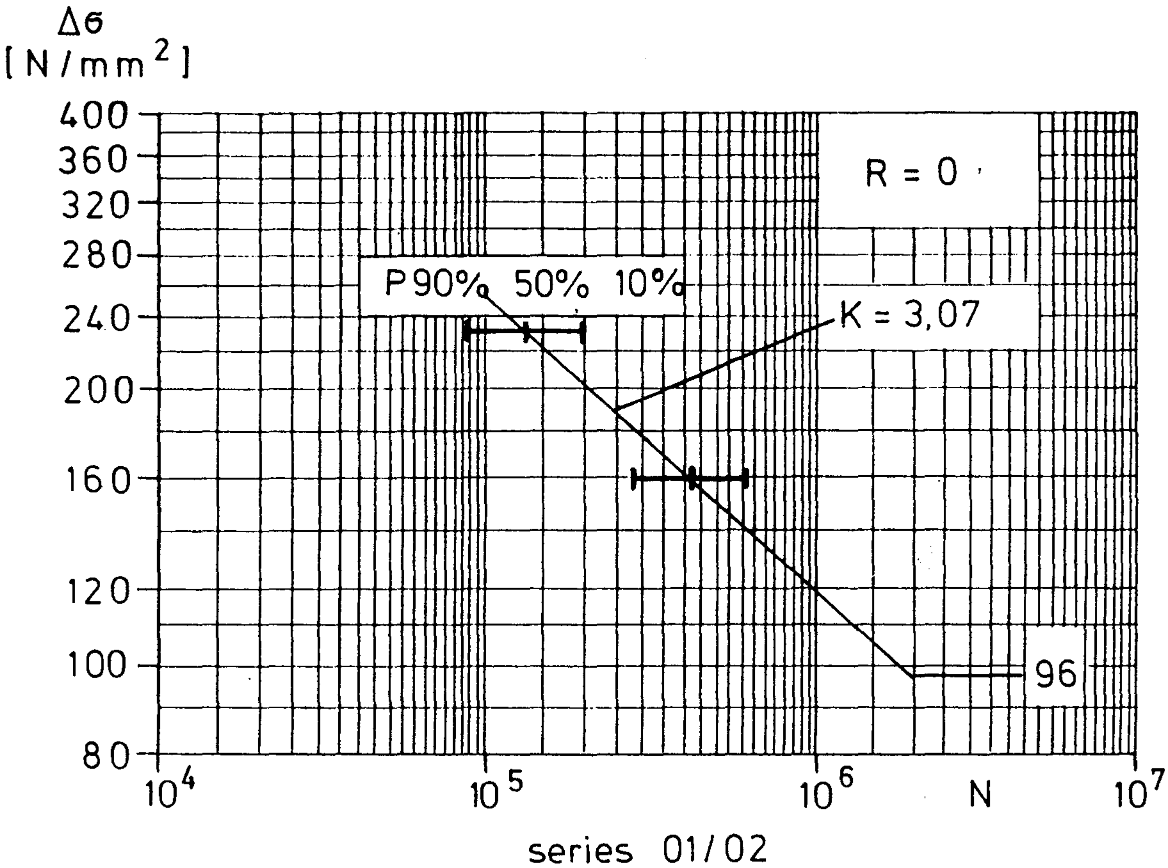

Fig. 9 S-N curve for zero-to-tension load

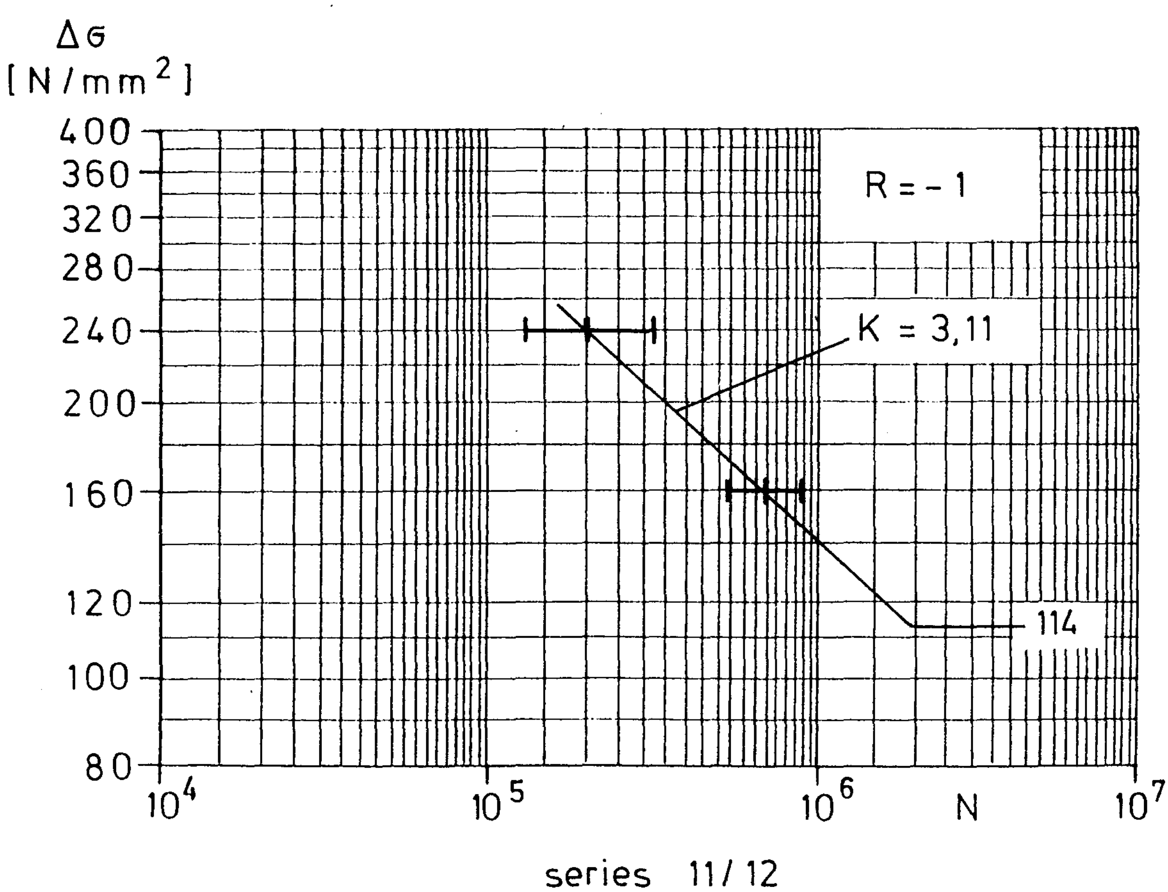

Fig. 10 S-N curve for alternating load

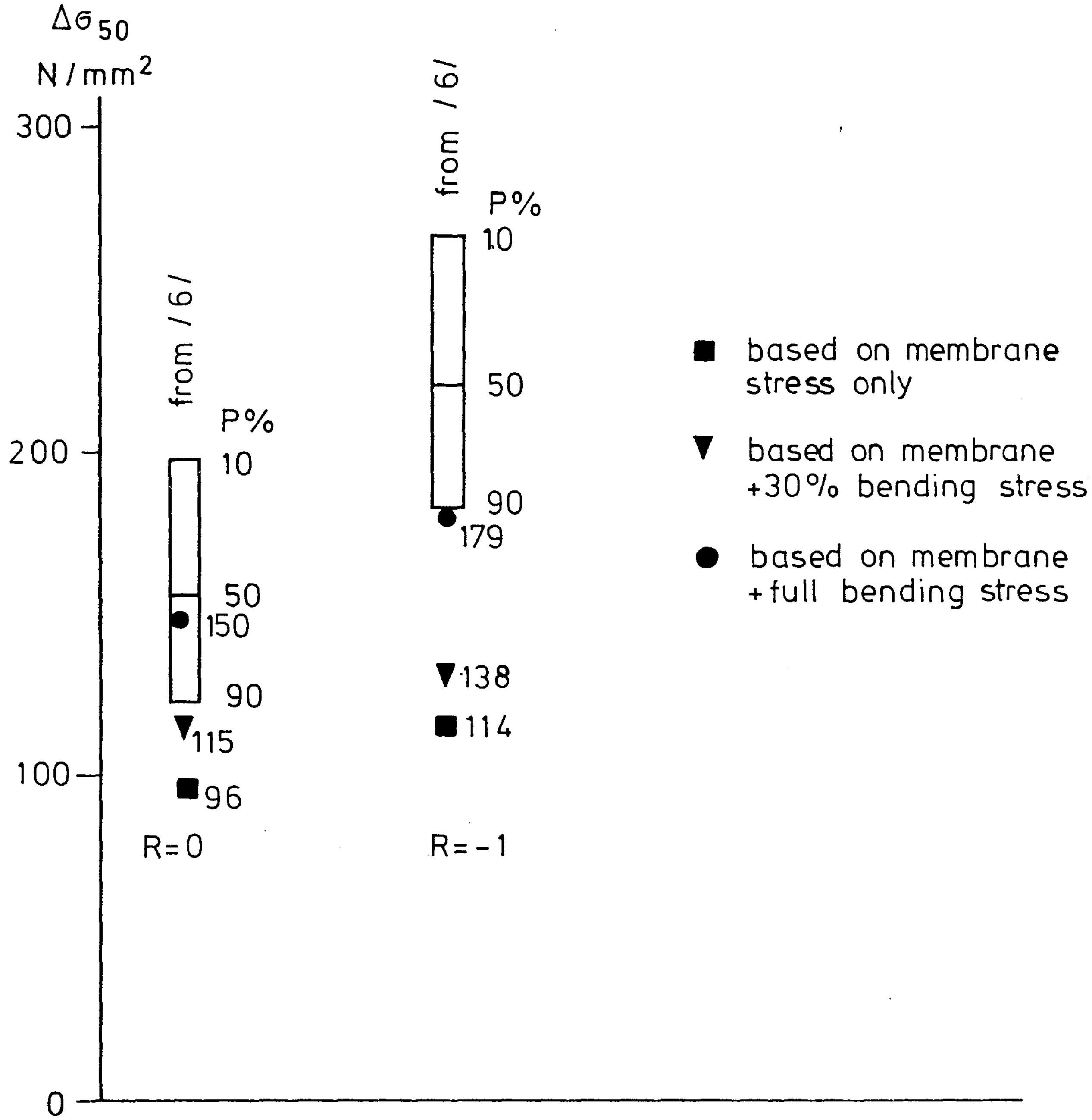

Fig. 11 Stress for 2 million cycles

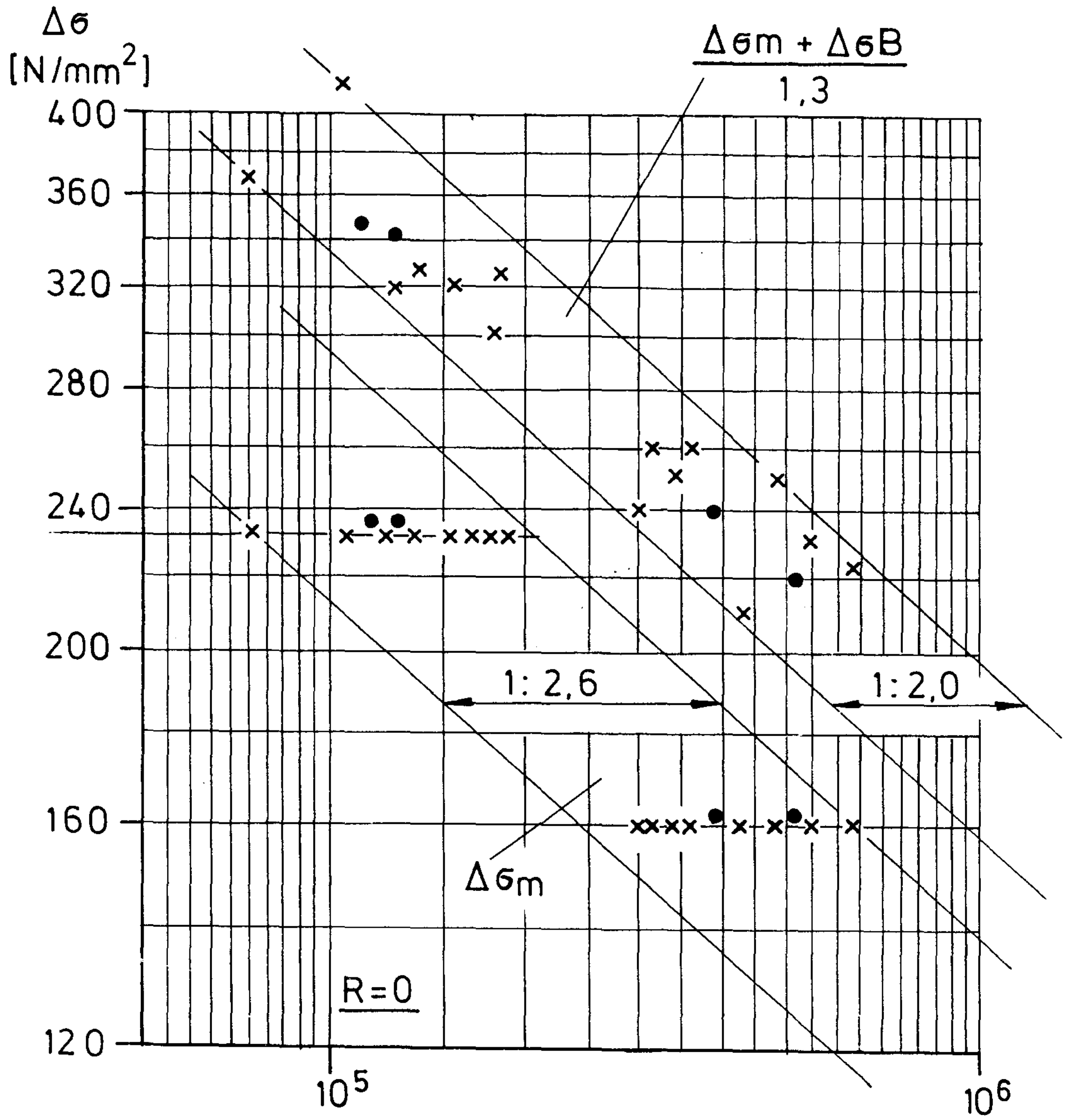

Fig. 12 Comparison of scatter bands for data from zero-to-tension load test

35

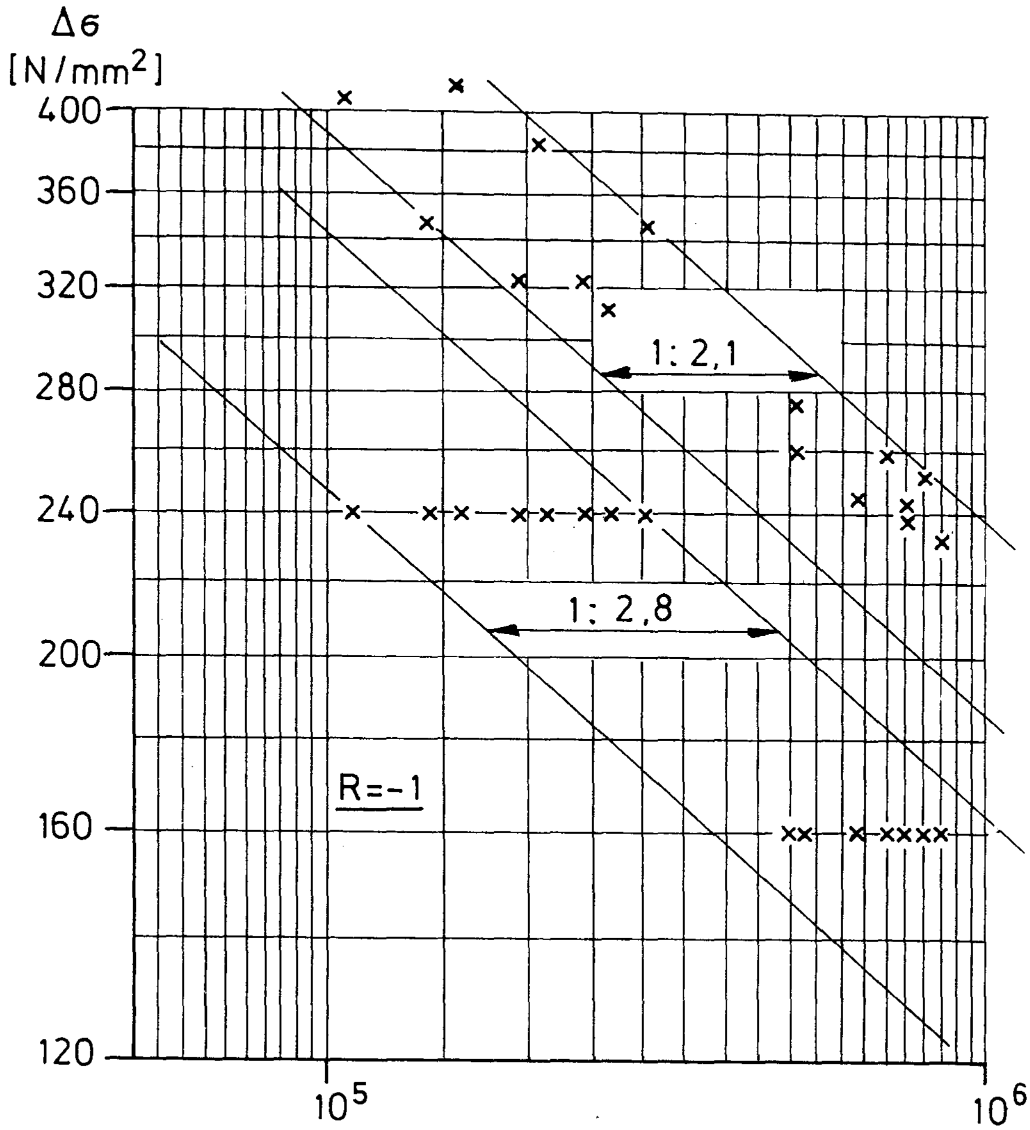

Fig. 13 Comparison of scatter bands for data from alternating load test

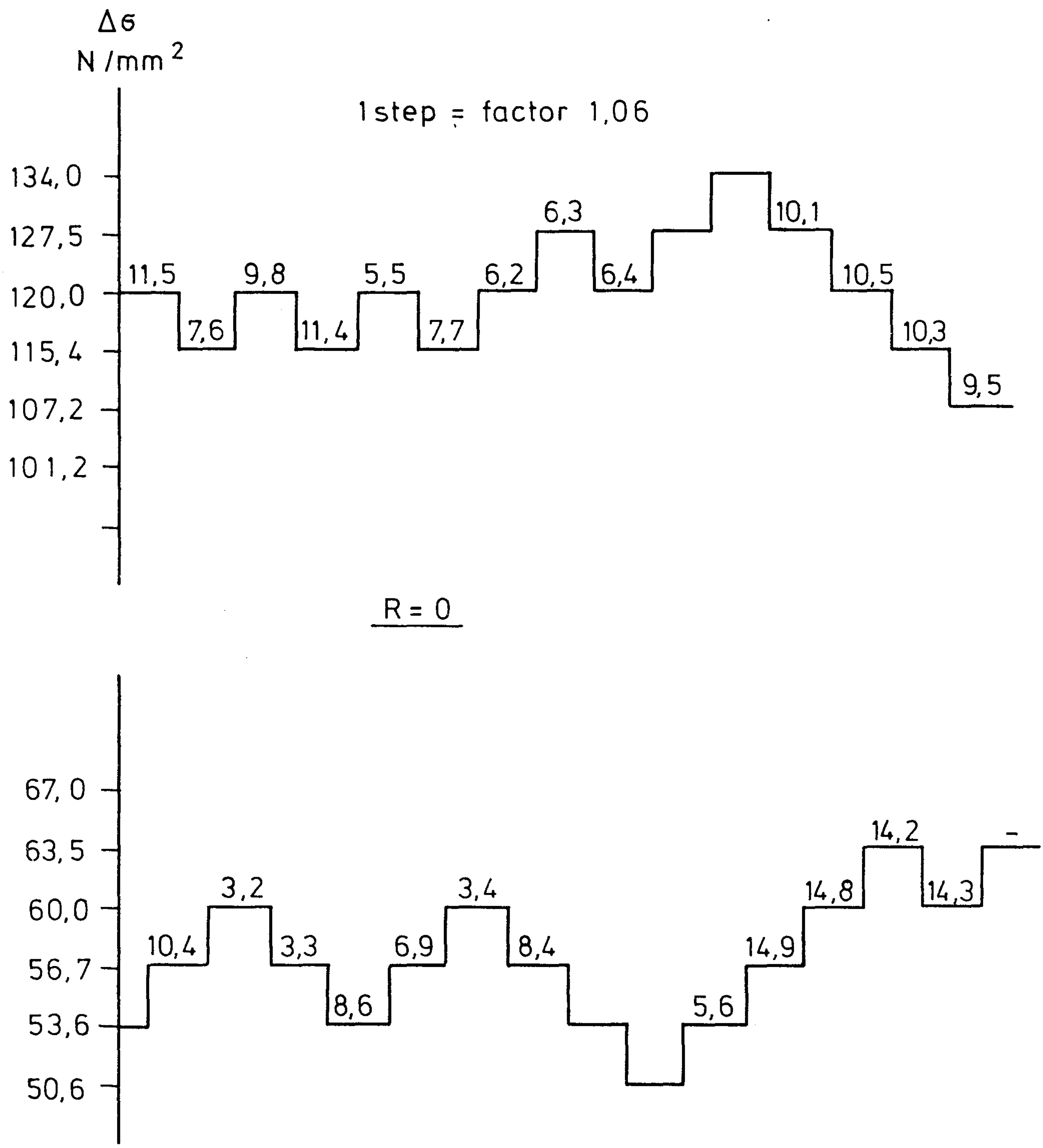

Fig. 14 Staircase test

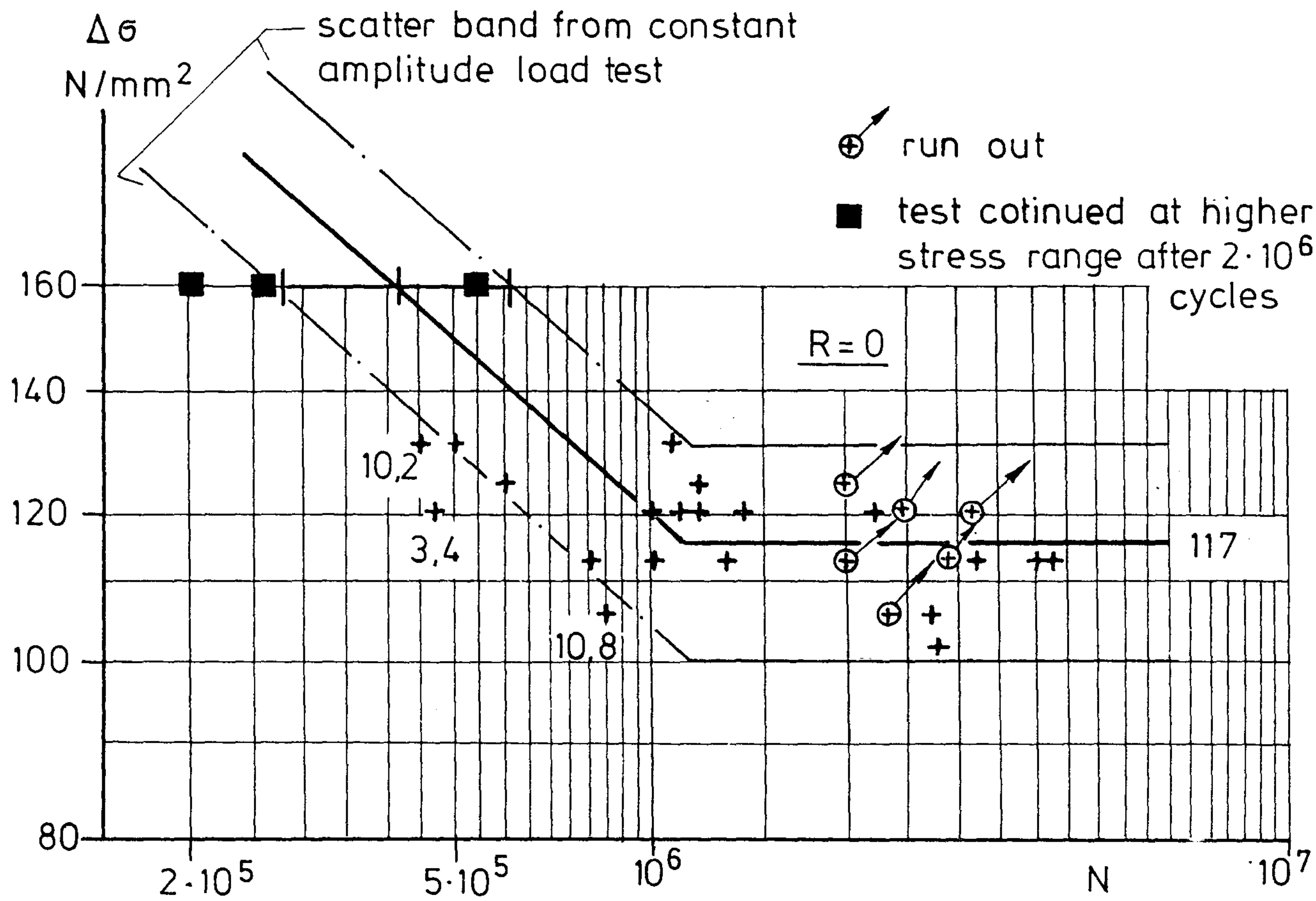

Fig. 15 Staircase test - individual test data

Specimen 1.2

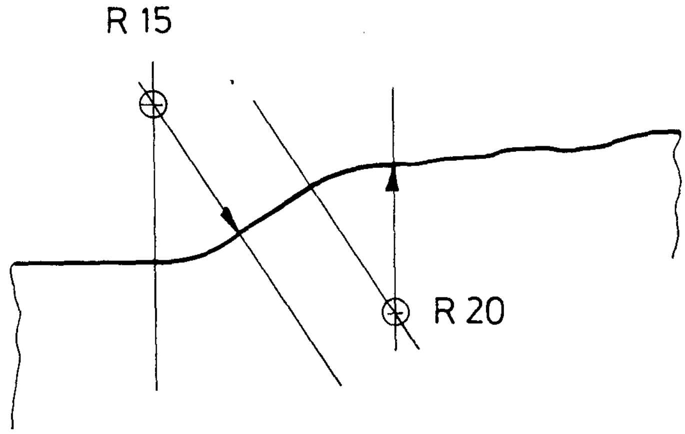

a) weld contour
10:1

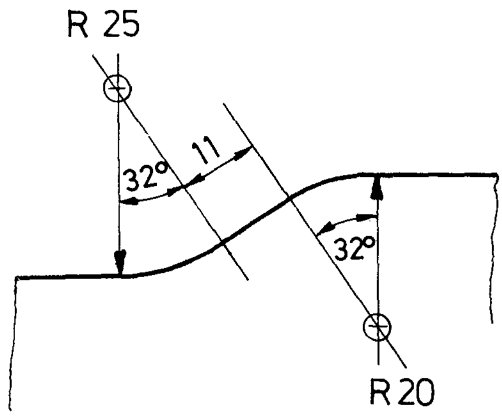

b) simplified weld contour
for calculation 10 : 1

Fig. 16 Weld contour for notch stress calculation

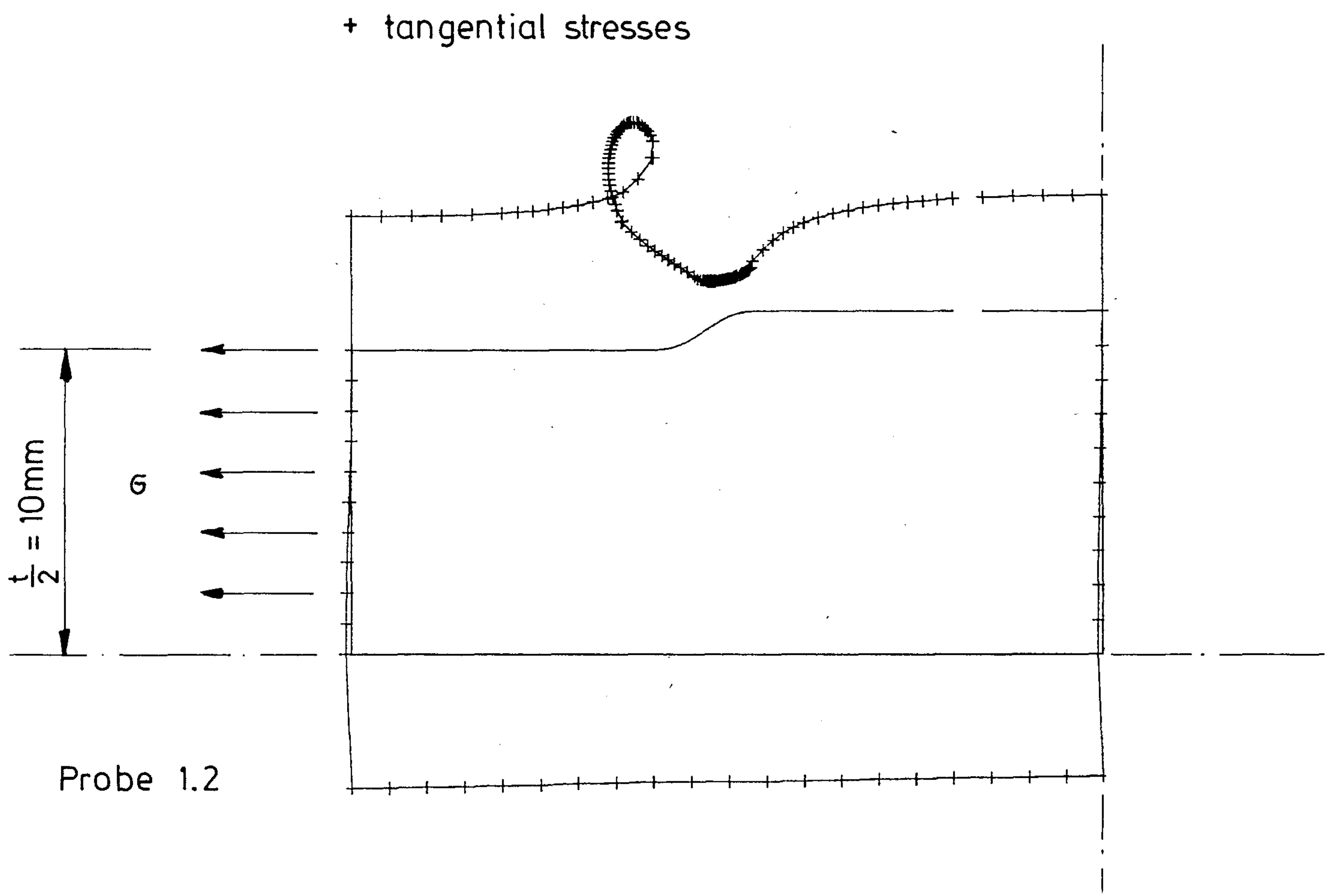

Fig. 17 Calculation model for notch stress calculation